12th International Symposium on Turbulence and Shear Flow Phenomena (TSFP12)
Osaka, Japan (Online), July 19-22, 2022

PIV MEASUREMENT OF TURBULENT FLOW AND PARTICLE MOTION OVER A ROUGH WALL

Kazumasa Matsumoto
Dept. of Civil and Earth Resources Engineering
Kyoto University
Kyoto 615-8540, Japan
email: matsumoto.kazumasa.85s@st.kyoto-u.ac.jp

Taka-aki Okamoto
Department of Civil Engineering
Meijo University
Nagoya 468-8502, Japan
email: okamotot@meijo-u.ac.jp

Michio Sanjou
Dept. of Civil and Earth Resources Engineering
Kyoto University
Kyoto 615-8540, Japan
email: michio.sanjou@water.kuciv.kyoto-u.ac.jp

ABSTRACT

To manage river environment, it is valuable to understand and evaluate the transport process of fine sediment and seeds of plants in a natural river since it can be one of the direct causes of development of riverine vegetation. In this study, two sets of laboratory experiments were conducted in a flume with a bed where hemispherical roughness elements were fixed in a staggered array to mimic a natural river. First, to investigate the structure of flow around the roughness elements, the velocity distribution near the roughness layer was measured by using particle image velocimetry (PIV). Results of PIV revealed structure of the mean and turbulent flow field around roughness, and also suggest that coherent motion of turbulent flows called sweep or ejection might play a significant role in mass transport process. Second, some particles were injected to the flow, and their motions near the rough bed were observed. Some trajectories of a particle indicate that the bursting events in the roughness sublayer are responsible for particle motions above and between roughness elements.

1. INTRODUCTION

Investigation of turbulent transport process of particles in an open channel is one of the most important topics in a wide range of fields of engineering. When it comes to civil engineering, for example, fine sediment and seeds of plants are conveyed by flow and deposited to riverbed in a natural river. Aquatic vegetation in a river channel plays an important role in determining the quality of riverine environment and the disaster risk of their basin. So, it is valuable to understand and evaluate the transport process of particles in a natural river which can be one of the direct causes of development of riverine vegetation.

The behavior of suspended particles in open channel flow is known to be strongly affected by the coherent structure of turbulent flows that develop near the bottom (Nino and Garcia, 1996; Cameron et al., 2020). It is well known that on a smooth wall, streaks of low momentum region induce the generation of hairpin vortex, and then instantaneous upward and down ward flows called ‘ejection’ and ‘sweep’ occur. Similarly, it has been pointed out that coherent structure may be formed over a rough wall. On the other hand, there are still few studies on the interaction between turbulence and behavior of suspended particles in a rough-wall flow.

In this study, two laboratory experiments were conducted in a flume with a bed where hemispherical roughness elements were fixed in a staggered array to mimic a natural river. First, to investigate the flow structure around roughness elements, the velocity near the roughness layer was measured by using PIV. Second, some spherical particles were added to the flow, and their motions near the rough bed were observed to investigate influence of turbulent flows on particle transport process. After these experiments, the results were compared with each other to reveal the interaction between the flow field and mechanism of particle transport.

2. EXPERIMENTAL METHOD

Figure 1(a) shows a schematic view of the experimental setup and the coordinate system. Experiments were conducted in a glass-made flume 10 m long, 0.40 m wide, and 0.50 m high. To mimic a gravel bed, hemispherical roughness elements, whose radius i.e. roughness k was 1.8 cm, were fixed in a staggered array over a 7 m area of the channel bed. In this study, two sets of experimental conditions are considered by changing the depth of flow H, as shown in Table 1. In both cases, the bulk mean velocity U_m was set to 0.30 m/s. The Reynolds numbers based on the mean velocity and flow depth $Re \equiv U_m H/\nu$ were 24,000 and 36,000.

The particle image velocimetry (PIV) is one of the most effective ways to visualize velocity distribution (Okamoto et al., 2021). To measure two-component instantaneous velocities (i.e. $\tilde{u}(t) \equiv U + u(t)$ and $\tilde{v}(t) \equiv V + v(t)$) by PIV, a 2.0 mm thick laser light sheet (LLS) was generated with a 3.0 W YAG laser source and projected into the channel. As shown in Figure 1(b), the lateral position of the LLS was at the center of the flume, where crests and valleys of roughness elements were located. A high-speed CCD camera (1280 pixel × 1024 pixel) at the side of the channel was used to take illuminated flow pictures in the measured cross-section. The size of the measurement area was 19 cm × 15 cm. The measurement area was located 3 m downstream from the upstream edge of the rough bed region where turbulence was fully developed.

In this study, particle motions around roughness were also observed. Some particles were introduced to the flow and their motions were recorded by two video cameras (3840 × 2160 pixels) installed at the side and above the flume. The particles were spherical, natural plant seeds with a mean diameter of 0.19 cm, specific gravity of 1.21 and settling velocity V_t of 5.2 cm/s.

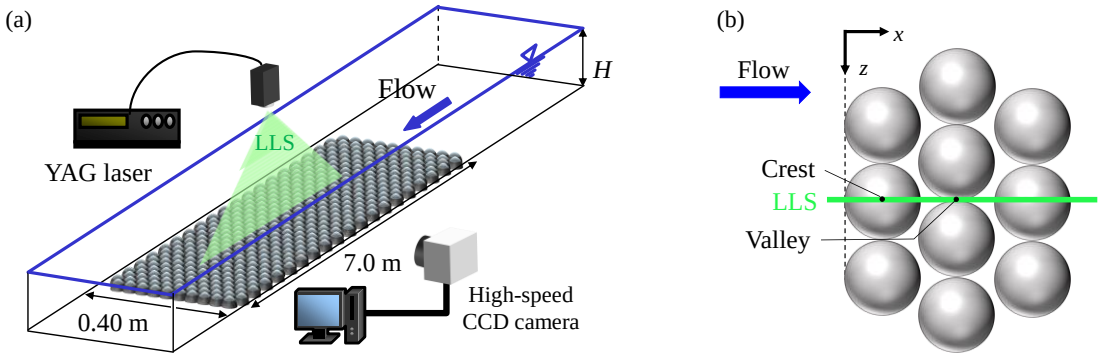

Figure 1. Schematic views of (a) experimental setup and (b) arrangement of roughness elements.

Table 1. Experimental conditions.

U_m [cm/s]	H [cm]	u_* [cm/s]	H/k	$Re \equiv U_m H/\nu$
30	8.0	4.0	4.4	24,000
30	12.0	3.6	6.7	36,000

Some of the particle trajectories were tracked over two sets of consecutive images. By combining horizontal (x-z) and vertical (x-y) trajectories obtained through the tracking procedure, some time-series of three-dimensional positions of a particle ($u_p(t)$, $v_p(t)$ and $w_p(t)$) were calculated. In addition, PIV was also conducted for the particle-laden flow to measure the flow structure around ascending or descending particles.

3. RESULTS

Mean and Turbulent Flow Structure

Results revealed structure of the flow field near the rough bed. Figure 2(a) shows the mean streamwise velocity profiles at the crest (x/k = 1.0) and valley (x/k = 3.0) of roughness (shown in Figure 1(b)). The values of velocity at the two measurement points are almost equal at each height except for the region near the roughness. In the vicinity of roughness height ($y/k \approx 1$), the streamwise velocities at the crest are reduced due to the effect of roughness, while those at the valley are relatively large. This demonstrates that flow separates from the roughness surface just downstream of the crest, where turbulence may be generated due to the velocity shear.

In this study, the friction velocities u_* were evaluated from the velocity profiles measured. It is known that the logarithmic law holds for rough-surface flows as follows,

$$\frac{\langle U \rangle}{u_*} = \frac{1}{\kappa} \ln\left(\frac{y - y_0}{k}\right) + B \qquad (1)$$

, where y_0 and B are the position of the virtual origin and the constant of the logarithmic law, respectively. κ is the von Kalman's constant, and in this study, $\kappa = 0.41$. The values of u_*, y_0 and B were calculated by fitting the logarithmic law to the measured velocity profiles. Figure 2(b) shows the velocity distributions $\langle U \rangle(y)$ for each case. The friction velocities for $H = 8.0$ cm and $H = 12.0$ cm are $u_* = 4.0$ cm/s and 3.6 cm/s, respectively, and the other values are $y_0 = 0.86k$ and $0.83k$,

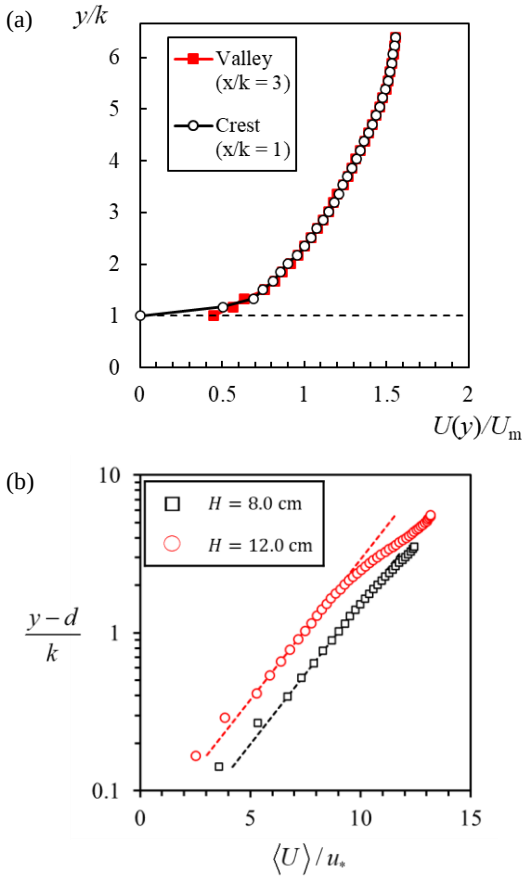

Figure 2. (a) Mean streamwise velocity profiles at the two locations shown in Fig.1(b) (x/k = 1.0 and 3.0, H = 12.0 cm), and (b) comparison of velocity profiles to the log law.

and $B = 8.9$ and 7.4, respectively. In both cases, the flow velocity profiles were found to be in good agreement with the logarithmic law in the range of $1.2 < y/k < 2.3$. In this study, this region is defined as the logarithmic layer, and the lower layer ($y/k < 1.2$) as the roughness sublayer. Raupach et al., 1991 defines flow field satisfying $k^+ > 70$ as fully rough flow. Thus, all cases in this study ($k^+ = 720$ and 650, respectively) can be classified as this flow regime.

Figure 3 shows a contour map of time-averaged vertical velocities V around roughness. In this graph, the black arrows denote time-averaged velocity vectors (U, V), and the dark-gray areas and the light-gray one correspond to roughness elements

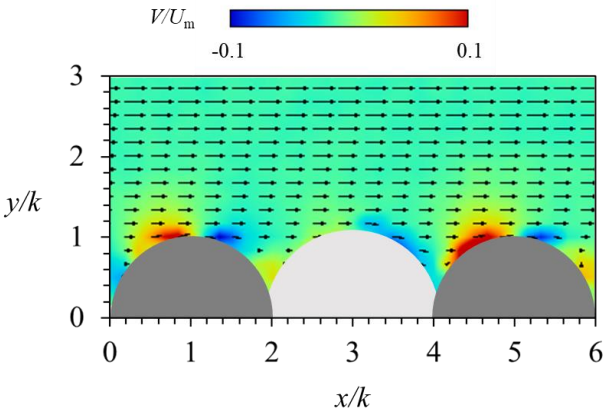

Figure 3. Contour map of mean vertical velocity V (H = 12.0 cm).

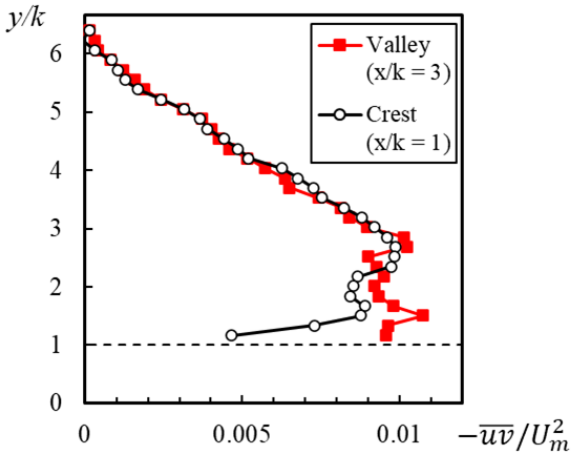

Figure 4. Vertical distributions of Reynolds shear stress $-\overline{uv}$ (H = 12.0 cm).

and an area behind roughness elements, respectively. Over the roughness ($y/k > 1.3$), the values of V are almost equal to zero and the flow field seems homogeneous. In contrast, around and below the roughness height ($y/k < 1.3$), remarkable positive and negative values of V are shown. At the roughness crests ($x/k \approx 1{,}5$), a pair of upward and downward flows is formed along the wall surface, while in the cavity ($3 < x/k < 4$), a downward flow intruding between roughness is observed. This is probably because drag force on streamwise flow by the roughness elements changes the flow direction. Although lateral velocities were not measured in this experiment, not only the vertical flows but also lateral ones should exist in this region due to the effect of the wall topography. Such heterogeneous velocity field around and within roughness is called roughness sublayer (Nikora et al., 2001), where particle motions transported by flow are expected to be significantly three-dimensional.

Such mean vertical flows are expected to partly affect the transport of particles into and from roughness sublayer. At the same time, since the magnitude of the wall-normal velocity is smaller than the settling velocity of particles V_t, the transport process around the rough wall seems to be strongly connected to turbulent structure as well.

Figure 4 shows vertical distributions of Reynolds shear stress $-\overline{uv}(y)$ at the crest ($x/k = 1$, white circles) and the trough ($x/k = 3$, red squares) of the roughness. In both the points, the values of $-\overline{uv}$ are smallest near the water surface and

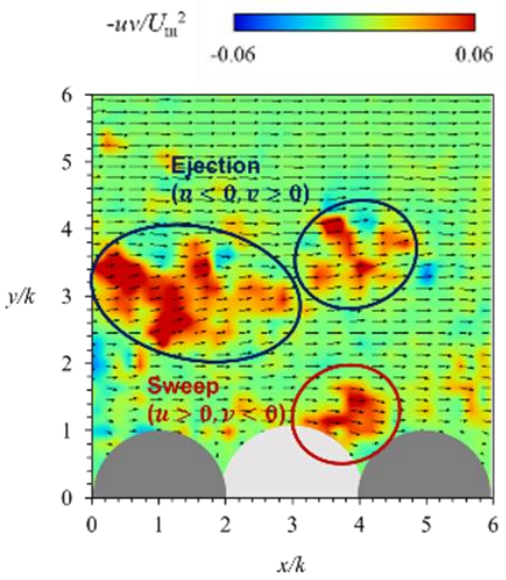

Figure 5. Contour maps of instantaneous Reynolds shear stress $-uv$. Black arrows denote instantaneous velocity vectors $(\tilde{u}, \tilde{v})$ (H = 12.0 cm).

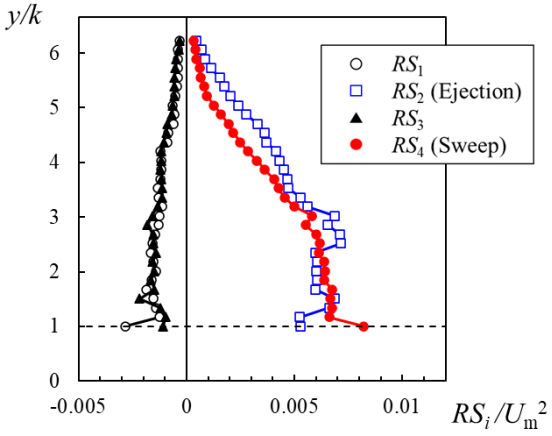

Figure 6. Vertical distributions of quadrant Reynolds shear stress RS_i at $x/k = 3$ (Valley, H = 12.0 cm).

increase almost linearly as approaching the bottom, which is a common tendency for an open channel flow. However, there is a significant discrepancy between the two graphs, especially around the roughness ($1 < y/k < 2$). At the crest ($x/k = 1$), the turbulent shear stress is steeply reduced in the vicinity of the bottom, which means production of turbulence is likely to be restricted in this region due to drag force of the roughness element. On the other hand, in the case of the trough ($x/k = 3$), the values of $-\overline{uv}$ are much larger than those in the case of the crest. This indicates that just downstream of the crest ($1 < x/k < 3$), turbulence is generated most actively in the flow since there is a large velocity shear due to flow separation.

Next, the turbulent flow structure over the rough bed will be further examined, which is expected to influence on the particle transport processes. Figure 5 shows a contour map of instantaneous Reynolds shear stress $-uv$ at a certain instance. The black arrows in the figure denote instantaneous velocity vectors $(\tilde{u}, \tilde{v})$. It is well-known that the coherent motions of

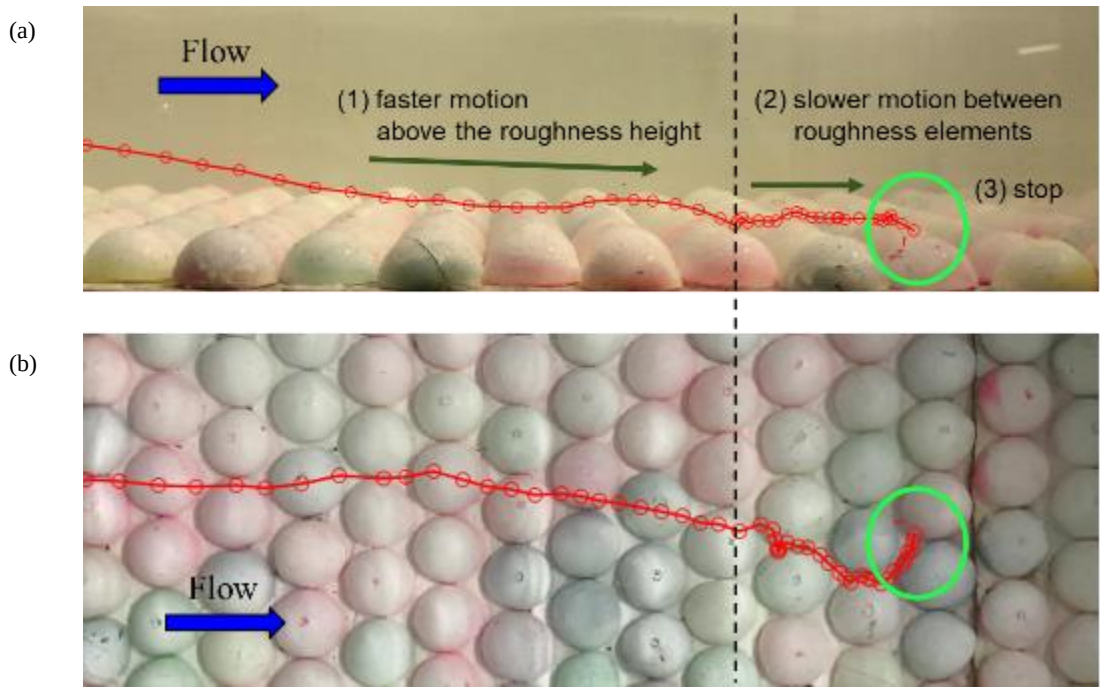

Figure 7. Example of the particle trajectories: (a) side view ($x-y$) and (b) top view ($x-z$) ($H = 12.0$ cm).

turbulent flows called ejection ($u < 0, v > 0$) or sweep ($u > 0, v < 0$) are observed in an open channel flow with roughness or vegetation (Bomminayuni and Stoesser, 2011). Occurrence of such turbulent events can be found from the results of velocity measurement by detecting positive values of $-uv$. In this contour, upward flow regions where the values of –uv are positive exist apart from the rough bed ($2 < y/k < 4$), corresponding to ejections. At the same time, a downward flow with high momentum, that is a sweep, occurs around and is about to intrude into the cavity between roughness elements. Okamoto et al., 2016 reported as to flow with submerged flexible vegetation that the coherent motions including sweep and ejection frequently penetrate into the upper part of a vegetation patch. These observations suggest that the intermittent upward and downward flows can be an important factor to determine particle trajectories around and over the roughness sublayer.

To explore the mechanism of momentum transport within and around the rough wall in more detail, a quadrant analysis was conducted for instantaneous Reynolds stress $-u(t)v(t)$ (Okamoto and Nezu, 2013). The quadrant Reynold stress RS_i is defined as follows:

$$RS_i = \lim_{T\to\infty} \frac{1}{T} \int_0^T \{-u(t)v(t)\} I_i(t) dt \qquad (2)$$

, where $I_i = 1$ if (u, v) exists in the *i*-th quadrant, otherwise $I_i = 0$. Figure 6 shows the vertical profiles of quadrant Reynolds stress RS_i at the valley ($x/k = 3.0$). Around the roughness height, contributions of the 2nd quadrant ($u < 0$, $v > 0$: ejection) and the 4th quadrant ($u > 0$, $v < 0$: sweep) to Reynolds shear stress exceed those of the other quadrants. This implies that the coherent structure develops and plays a significant role in mass and momentum transport in this region. What is more, this graph indicates that ejection contributes to Reynolds stress more than sweep near the water surface while the 4th quadrant event is more active around roughness. These tendencies agree with results of numerical analysis of flow over a cubical roughness by Coceal et al., 2007. Thus, it is necessary to understand relationship between turbulent structure and transport process of particles over a rough wall.

Influence of Turbulence on Particle Motions

Figure 7 shows an example of the particle trajectories in vertical and horizontal planes observed in this experiment. The particle fell down outside the roughness sublayer, and repeated small upward motions and downward ones several times around the roughness height ($1 < y/k < 1.5$), which corresponds to (1) in the photos. It seems that this motion was caused by the mean vertical flows formed along the roughness surface shown in Figure 3 or by coherent motions of flows in the roughness sublayer illustrated in Figure 5 and 6. After the faster motion above the roughness height (1), the particle passed through the roughness elements with slower speed and finally stopped, which corresponds to (2) and (3). This implies that unless any sufficient upward force by fluid acts on a particle floating around the roughness height, it falls into the cavity of roughness and becomes easy to be trapped between roughness elements. Moreover, it was also observed in another example of the particle trajectories that a particle once trapped was re-suspended and flew out of the rough wall. This observation suggests that such an intermittent motion in the wall may be connected to the momentum transport process by sweep and ejection indicated in Figure 6.

Figure 8 shows a series of instantaneous velocity fields when a particle is ejected from the cavity of roughness and ascending to the outer flow region. Here, contour and arrows show distribution of instantaneous Reynolds stress $-uv(t)$ and velocity fluctuation vectors (u, v), respectively. The white circle is the position of a particle at the moment ($t = 0.30$ s), and the black dashed lines correspond to the particle trajectory before and after the instant.

The present observation indicates the coherent structure of turbulent flow is likely to cause particle entrainment from the

(a) $t = 0$ s (The particle exists within roughness.)

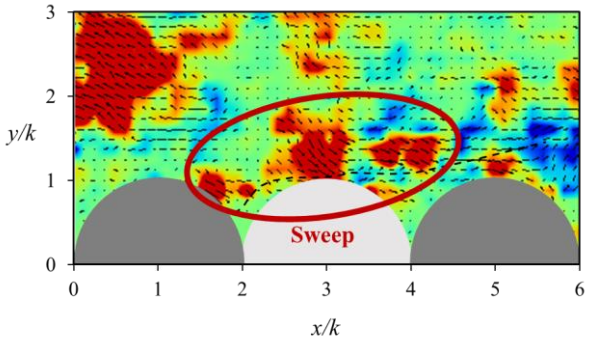

(b) $t = 0.3$ s (The white circle denotes the particle position.)

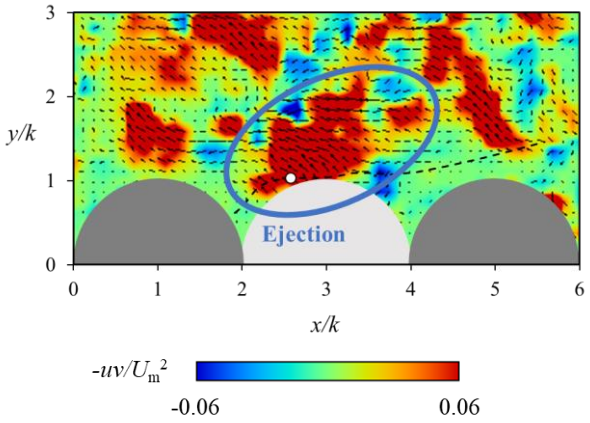

Figure 8. Contours of instantaneous Reynolds stress $-uv(t)$ with velocity fluctuation vectors (u, v). The dashed black lines denote the particle trajectory before and after each moment ($H = 8.0$ cm).

rough wall. In Figure 8(a), downward flow with high momentum occurs just above roughness and penetrates into cavity of the rough wall. And 0.13 s after this moment, the particle emerged from roughness and started to ascend into the outer flow. As shown in Figure 6, transport of the high-momentum flow is significant near and maybe below the roughness height ($y/k \approx 1$). So, sweep ($u > 0$, $v < 0$) seems to be a key factor to evoke particle entrainment and lift-up from roughness sublayer into the flow. In other words, the bursting phenomena over a rough wall may play a significant role in determining the transport process of particles within and around the roughness layer.

Figure 8(b) illustrates that an instantaneous upward motion of flow with low momentum ($u < 0$, $v > 0$) is occurring in the vicinity of the ascending particle. Also, at this moment, the ejections occur not only just around the particle, but also in a wide area above the roughness. This implies that the particle upward motion starting near the roughness height may occur if the particle gets captured in the low momentum region (LMR) above roughness and instantaneous upward flow.

To evaluate length scale of particle motions over the rough bed, step lengths of particles were calculated from the trajectories observed in this experiment. In this study, the length is defined as a distance that a particle travels since it starts to move in the streamwise direction until it stops between roughness elements (Liu et al., 2019). Figure 9 shows histograms of step length L for all cases ($H = 8.0$ cm and $H = 12.0$ cm). The numbers of samples obtained in the experiments were 81

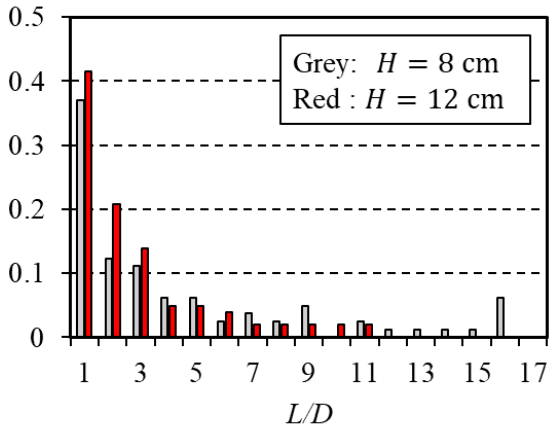

Figure 9. Histograms of particle step-length L for $H =$ 8.0 cm and 12.0 cm.

and 101. Here, the values of L is divided by the diameter of hemispherical roughness elements, L/D, and the average values Λ/D were 4.5 and 2.9, respectively. The distribution of L/D covers a wide range of values from one to more than ten in each case. This variation in the values might be attributed to the occurrence of instantaneous upward flows, that is to say ejections. Comparing the two cases, it can be observed that the averaged step-length is longer in the lower depth case ($H =$ 8.0 cm) than that in the other case. This may be because turbulence is generated more actively in the former case due to larger friction velocity and particles are lifted up by upward flow around roughness for a longer period of time.

In the end, a conceptual model of particle transport process over a rough wall obtained from the results of this study is proposed. As well as ejection, sweep may affect the particle transport within roughness since it is the most significant event as to momentum transport in this region, as shown in Figure 6. Van Hout, 2013 pointed out that in open channel flow over a smooth wall, a particle on the wall gets suspended just after a high-speed fluid reaches the wall. This mechanism of the particle entrainment might be applied to the rough wall flow although its flow structure is quite different from that of a smooth wall. However, most of the flow field in the cavity of roughness could not be measured and still unrevealed in this experiment. The interaction between coherent structure and particle transport process within the rough wall should be explored in the future work. Just after the particle lift-up, if upward transport of low-speed fluid occurs around over the roughness height, a particle tends to be lifted up and transported over roughness for a long period. Otherwise, a particle cannot ascend high enough to reach the outer region of roughness and go back into the cavity quickly.

4. CONCLUSIONS

In this study, the results of PIV revealed the mean and turbulent flow structure over a hemispherical rough wall. Topography of the wall causes flow separation from the roughness surface and large velocity shear around the roughness height. This strong shear generates turbulence and forms coherent structure of turbulent flows, which contributes to mass and momentum exchange within and around the roughness sublayer. Moreover, observation of particle motions and their comparison to the results of velocity measurement show that the

bursting phenomena, including upward and downward flows called ejection and sweep, can be a trigger of the suspension process of particles within and above a rough bed.

REFERENCES

Bomminayuni, S., and Stoesser, T., 2011, "Turbulence statistics in an open-channel flow over a rough bed", *J. Hydraul. Eng.*, 137(11), 1347-1358.

Cameron, S. M., Nikora, V. I. and Witz, M. J., 2020, "Entrainment of sediment particles by very large-scale motions", *J. Fluid Mech.*, Vol. 888, A7.

Coceal, O., Dobre, A., Thomas, T. G. and Belcher, S. E., 2007, "Structure of turbulent flow over regular arrays of cubical roughness", *J. Fluid Mech.*, Vol. 589, pp.375-409.

van Hout, R., 2013, "Spatially and temporally resolved measurements of bead resuspension and saltation in a turbulent water channel flow", *J. Fluid Mech*., vol.715, 389-423.

Liu, M.X., Pelosi, A., and Guala, M., 2019, "A statistical description of particle motion and rest regimes in open-channel flows under low bedload transport", *Journal of Geophysical Research: Earth Surface*, 124, 2666-2688.

Nikora, V., Goring, D., McEwan, I., and Griffiths, G., 2001, "Spatially averaged open-channel flow over rough bed", *J. Hydraul. Eng.*, 127(2), 123–133.

Nino, Y., and Garcia, M.H., 1996, "Experiments on particle-turbulence interactions in the near-wall region of an open channel flow: implications for sediment transport", *J. Fluid Mech*., vol.326, 285-319.

Okamoto, T. and Nezu, I., 2013, "Spatial evolution of coherent motions in finite-length vegetation patch flow", *Environ Fluid Mech*, Vol.13, pp.417-434.

Okamoto, T., Nezu, I., and Sanjou, M., 2016, "Flow-vegetation interactions: length-scale of the 'monami' phenomenon", *Journal of Hydraulic Research*, 54(3), 251-262.

Okamoto, T., Tanaka, K., Matsumoto, K., and Someya, T., 2021, "Influence of velocity field on driftwood accumulation at a bridge with a single pier", *Environmental Fluid Mechanics*, 21(3), 693-711.

Raupach, M. R., Antonia, R. A., and Rajagopalan, S., 1991, "Rough-wall turbulent boundary layers", *Applied Mech. Rev., ASME*, vol. 44, 1-25.